Pergamon

Journal of Structural Geology, Vol. 16, No. 9, pp. 1283 to 1296, 1994

0191-8141/94 $07.00+0.00

0191-8141(93)E0028-J

Crystal growth during a single-stage opening event and its implications for syntectonic veins

C. J. L. Wilson

School of Earth Sciences, University of Melbourne, Parkville, Victoria 3052, Australia

(*Received 7 December* 1992; *accepted in revised form* 29 *November* 1993)

Abstract—The crystallization of a fluid filled vein or cavity and interpretation of the microstructure in a deformed rock is an important problem for geologists. Dynamic crystallization experiments using ice and an aqueous solution have been used as an analogue system for single-stage opening events and have shown that the presence or absence of a deviatoric stress is an important factor in the development of texture as a result of crystallization from a fluid. The textures can vary from (1) coarse crystal aggregates involving static growth where there is no significant macroscopic deviatoric stress at the time of crystallization, the *free-face growth model* to (2) polycrystalline aggregates involving static growth which develop from a mixture of skeletal crystals and fluid in a stressed environment. In the latter situation, the crystals and fluid coexist until the macroscopic stress can be transmitted between impinging crystals and, at this stage, fast dynamic recrystallization and grain boundary migration occurs. This recrystallization has been termed the *contact growth model* and the resulting metamorphic texture is compared with examples in natural quartz veins. During a single stage vein opening, uncomplicated by intragranular deformation, either free-face and/or contact growth textures can develop from the fluid filled void depending upon the kinematic environment.

INTRODUCTION

SYNTECTONIC vein systems in deformed greenschist and lower grade metamorphic rocks contain a variety of internal microstructures. These veins are generally considered to form by hydraulic fracture processes at near lithostatic fluid pressures and where there are low stress differences ($\sigma_1 - \sigma_3$) (Etheridge 1983), followed by hydraulic fluids involved in the crystallization of minerals such as quartz or calcite in the fracture. Microstructures in such veins can indicate the nature of the crack opening, which may be either single stage or by crack–seal events (Durney & Ramsay 1973, Ramsay 1980). A single-stage opening of a vein involves the formation of a fluid-filled cavity, followed by crystallization that is not accompanied by further micro-fracturing. This type of vein growth produces complex vein microstructures (Fig. 1) which include massive grain aggregates with equant growth habits (Beach, 1977), ingot textures and euhedral crystals (Downing & Morrison 1989), fibrous microstructures at vein margins (Durney & Ramsay 1973) or coarser grained anhedral veins that may contain comb structures and crustification textures (Downing & Morrison 1989).

A vein that has experienced a single-stage opening event may also be followed by further fracturing and vein infilling in response to localized stress conditions. This will result in the development of other microstructures, the nature of which will depend on the prevailing macroscopic stress field. The macroscopic state of stress, which represents the overall forces experienced by the rock on the scale of many grains, is quite different from the microscopic stresses existing within a grain crystallizing from a fluid. The microscopic stresses depend on individual crystallographic orientations and are dominated by differing crystal elastic energies, surface energies and crystal–fluid interfacial energies (Wheeler 1991). When there is fluid flow through rocks undergoing metamorphism, it is the microscopic stresses that govern initial textural equilibrium. The geometry of fluid-filled pores or cavities in a solid, and hence the permeability of the solid, is controlled by the dihedral angle of the fluid against the solid. Although it is known that the dihedral angle is modified by changes in fluid composition in an environment of no applied macroscopic stress (Holness & Graham 1991) there are few studies that investigate how the dihedral angle and the equilibrium textures relate to changes in the state of stress. In this paper it is proposed to use experimental observations to gain an insight into the origin of contrasting microstructures that develop when a mineral grows in a fluid-filled environment such as a vein opening and is then subjected to a macroscopic stress. It is intended to specifically investigate the formation of a single-stage vein system where: (1) the sealed vein is in equilibrium with the macroscopic deviatoric stress; and (2) the sealing of the vein and the transmission of a deviatoric stress across the vein is such that it is not in equilibrium with the deviatoric stress.

EXPERIMENTAL PROCEDURE

Experimental methods

The experiments were performed in the apparatus described by Wilson (1984). Three experiments are illustrated in this paper (Figs. 2 and 3) that involved two ice-crystal types: (1) large elongate crystals that are separated by smaller crystals (Fig. 2a). This has been produced by crystal growth parallel to a frozen surface and is similar to the ice prepared by Wilson (1981); and (2) polycrystalline ice (Fig. 3a) that contains equant grains with randomly oriented *c*-axes similar to the ice described by Wilson (1986). The sample (approximately $40 \times 20 \times 0.7$ mm) was deformed between two glass plates by driving a 0.7 mm thick platen into one end of the sample to achieve a strain rate of $9.7 \times 10^{-5}\ s^{-1}$. Dynamic events in the deforming specimen were recorded in transmitted polarized light either on a 35 mm film or using a time lapse camera on 16 mm film over periods of approximately 3.4×10^5.

The lower and upper surfaces of the sample were lubricated with a film of silicon oil and during the deformation the sample was contained in a silicon oil bath. The temperature of the silicon oil was maintained at -1 ± 0.01°C by circulating air around the specimen within an insulated container. A single-stage melting event was induced as a result of deformation and occurred in selected areas within the sample. This produced voids that were filled with water. Lateral motion of the fluid was restricted by either the framework of host grains or a film of silicon oil on the boundaries of the sample, which meant that the experiments were essentially constant volume.

Temperature decreases that induced crystallization in experiments F2 and M14 were obtained by varying the balance between a platinum resistance thermometer bridge and a set of heaters attached to the air circulating fans. As soon as melting was observed, the circulating air was instantaneously cooled to lower than -1°C and subsequently maintained at a temperature of -1°C. In experiment F3, melting and crystallization occurred at -1 ± 0.01°C and was only discovered after the film recording the experiment was processed. The existence of local pools of melt persisted in these experiments for up to 40 h, however, crystallization generally occurred in intervals of less than 30 min.

Two modes of ice crystallization that involved the presence of absence of a macroscopic deviatoric stress were observed in these experiments. These were related to the motion of the end platen and involved: (1) static crystallization where there was no deviatoric stress and no deformation as the platen was stopped at the onset of crystal nucleation; and (2) deformation continued both during the presence of a fluid phase and after crystallization.

Boundary conditions

The thickness of the sample was kept approximately constant by the covering glass plates. This can be seen in the negligible change of the second-order birefringence colours in all solid phases from the initial to the final stages of deformation (Figs. 2 and 3). During deformation, there was local melt observed by the marked birefringence changes and formation of water (black areas in plane-polarized light). However, the melt was contained between the glass cover plates so that the deformation at all times was essentially plane strain.

Translation of the movable platen under conditions of plane strain produces a shortening of the sample. With deformation involving $\leq 10\%$ longitudinal shortening, there was clear evidence that the deformation involved pure shear. To accommodate the plastic deformation, the unconstrained boundaries moved outwards at a near uniform rate. However, between 10 and 30% shortening, there was a noticeable departure from pure shear with the width of the sample increasing adjacent to the fixed platen. This is analogous to what is happening, where a flat indenter is pushing ductile material towards a rigid boundary (Tapponnier & Molnar 1976). The corresponding slip-lines (Fig. 4) are shear trajectories along which there is a tangential component of displacement with pure shear occurring on, or parallel to, the slip-lines (Johnson & Mellor 1973). The actual shape of the boundaries of the sample, and hence the boundary conditions, change as deformation progresses, and Fig. 4(a) is an example of the slip-lines only appropriate for the onset of yielding. As predicted by the theory (Johnson & Mellor 1973), there will be a dead triangular area (ABC in Fig. 3a) formed between a set of conjugate shears and the moving platen. Lateral extrusion along the free boundary of the plastically deformed material will be greatest in front of the fixed platen and will progressively decrease towards the conjugate shears.

EXPERIMENTAL RESULTS

Plastic deformation prior to melting

Figures 2 and 3 illustrate the general sequence of deformation recognized. The thin layers of ice initially deformed homogeneously on the sample scale, and the first changes were obvious grain boundary adjustments (Figs. 2a and 3a & b) with the development of sutured grain boundaries. These occur by migration of the original boundaries contemporaneous with the development of slip bands parallel to (0001). The presence of slip bands diminishes as there is a gross change of crystallographic orientation and grain boundary migration becomes dominant. This is particularly obvious in the finer grained polycrystalline aggregate (Fig. 3) where crystals with *c*-axes that are initially oriented either at a low or high angle to the shortening direction become progressively smaller and are removed from the sample. Prior to the onset of any obvious melting, the polycrystalline samples consisted of coarse interlocking grains with a strong crystallographic fabric, determined from birefringence variations. The *c*-axis pattern in such samples is typically a double maxima lying between the 25° and 50° small circle girdles about the shortening axis as described by Wilson (1986).

In the coarser grained sample (Fig. 2) there is an increasing misorientation within some individual grains followed by migration of the boundaries (arrow on boundary of grain a in Figs. 2a & b). Slip lamellae develop in some grains at the onset of deformation (grain b, Fig. 2a) but evidence for their existence be-

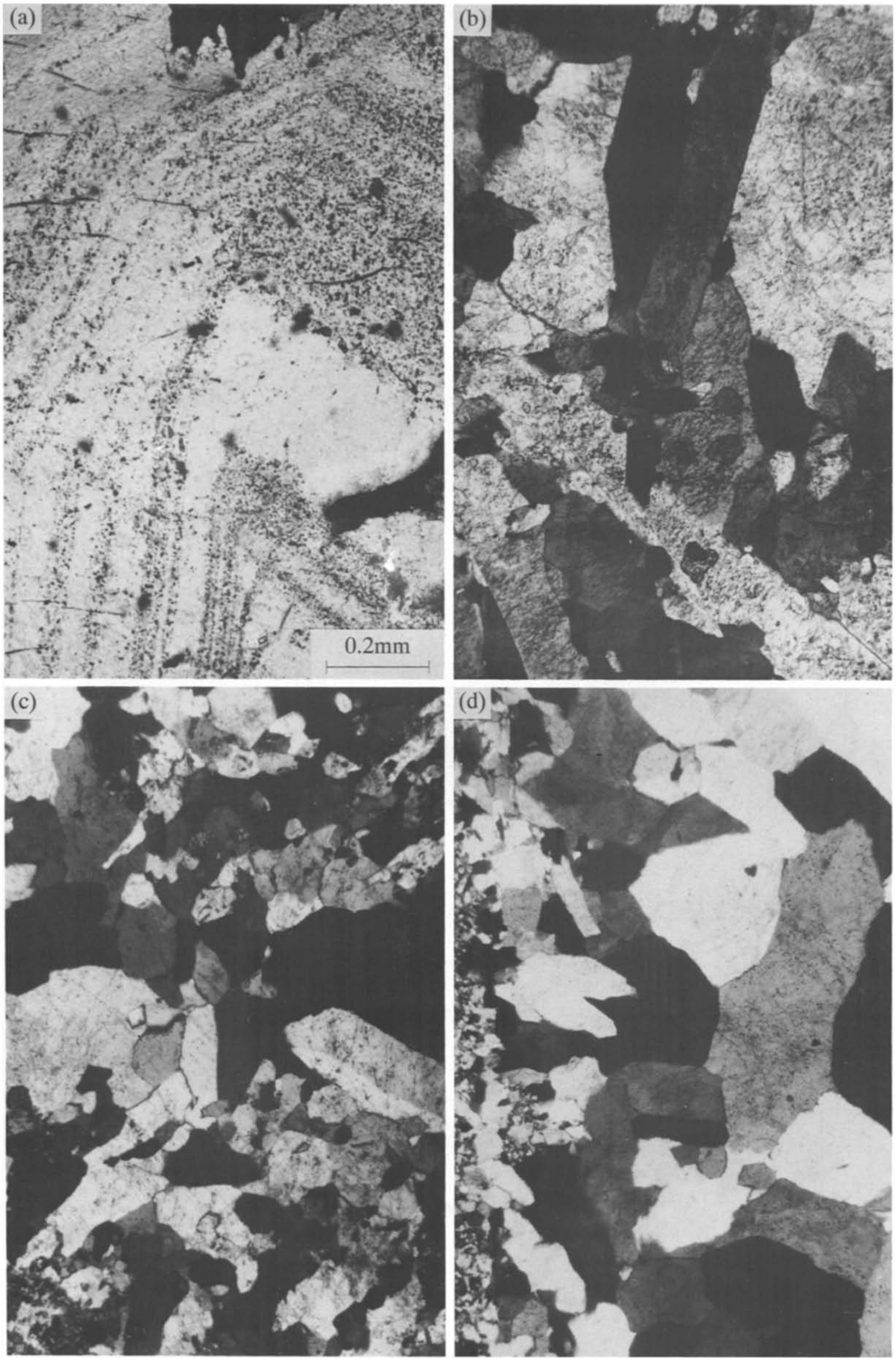

Fig. 1. Micrographs that illustrate natural quartz vein textures. (a) Free-face crystal growth from a fluid-filled vein (from Zermatt, Switzerland). (b) Elongate grains produced in a dilational vein that is infilled with crystals that display free-face growth textures (from Walhalla, Australia). (c) Variation in grain sizes and orientations as a result of free-face growth (from Walhalla, Australia). (d) Transition from wallrock through a zone of free-face to contact growth textures (from Walhalla, Australia). The magnification of each micrograph is as shown in (a).

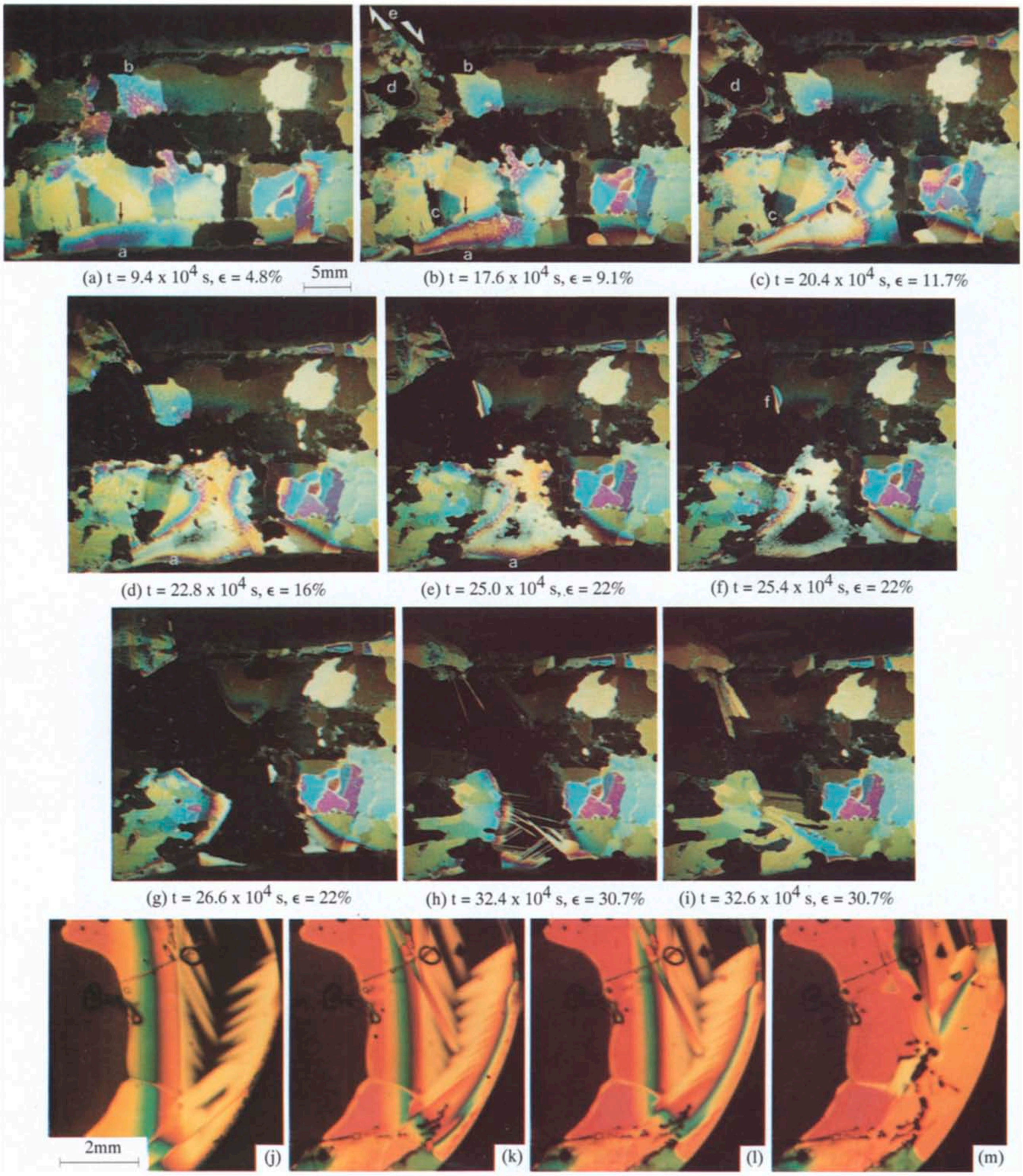

Fig. 2. Crystallization from fluid with no deviatoric stress ($\Delta\sigma = 0$). (a–f) The microstructural evolution during the deformation and accompanying melting in coarse ice aggregates involving a horizontal shortening by a rigid platen acting horizontally on the right-hand side of the sample (experiment F2). The time (t) in s $\times$ 10^4 and the corresponding average percent longitudinal shortening strain (ε) are shown beneath the representative stages in the textural evolution. (g) The last stage of melting prior to turning off the motor drive. (h&i) Free-face growth of ice from melt with no deformation. (j–m) Shows details of the crystal growth processes from a fluid, with no stress, and the formation of an interlocking crystal aggregate. The dark areas on the crystals represent silicon oil bubbles trapped between the ice and the constraining glass plates.

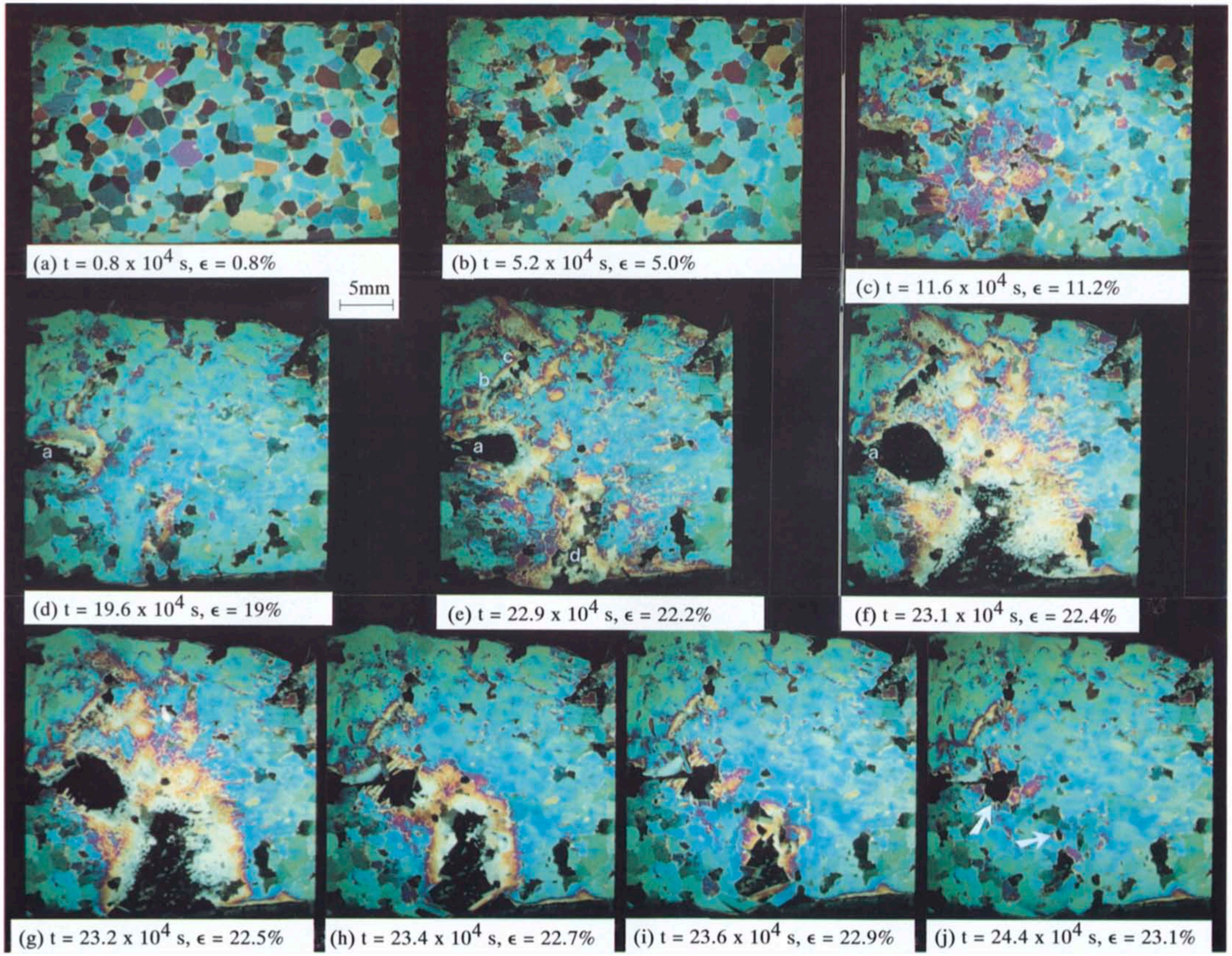

Fig. 3. Crystallization with a deviatoric stress ($\Delta\sigma \neq 0$). (a–c) Typical progressive shortening and microstructure evolution in polycrystalline ice aggregates with *horizontal shortening* from right to left (experiment F3). The time interval (t), in s $\times$ 10^4 and average percent longitudinal shortening strain (ε) are shown beneath the representative stages of textural evolution. (d–f) The progressive development of a melt region. (g–j) Crystal growth of ice in a deviatoric stress field (experiment M14).

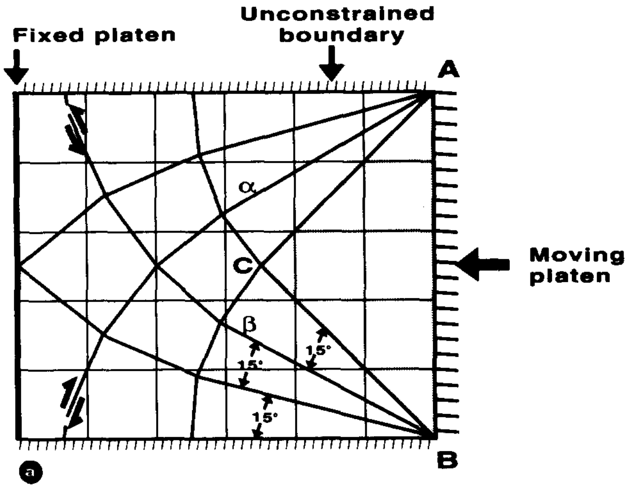

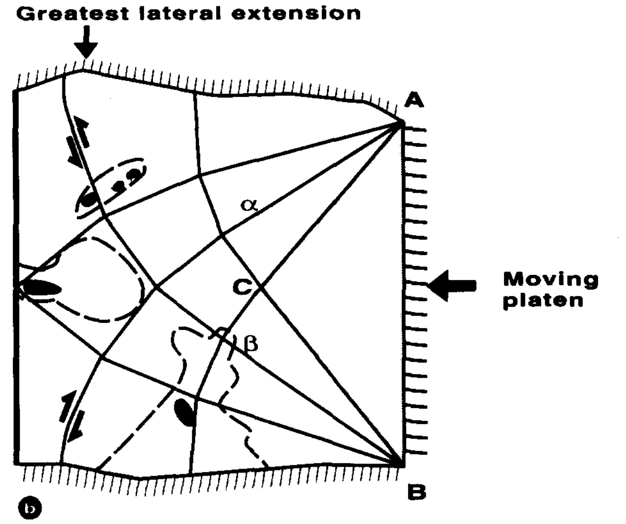

Fig. 4. An approximated slip-line field for plane strain indentation of a plastic medium. (a) Following convention (Johnson & Mellor 1973) the 15° equiangular set of slip-lines radiating from A are α-lines and those from B, β-lines and differ only in sense of movement and bound an area (ACB) which is a zone of higher normal stresses. (b) The slip-line field superimposed on stage (d) of Fig. 2, which corresponds to the onset of melting. It should be noted that the sites for the initial melting (shown in black) lie close to slip-line trajectories that correspond to areas of maximum resolved shear stress. The broken line shows the final distribution of fluid (Fig. 2g) at the onset of crystallization.

comes less as grain boundary migration begins to dominate. In other grains, after a gentle crystal lattice bending, new grain boundaries start to evolve (area c, Fig. 2c) and develop small new grains that overprint and destroy the original grain structure. The degree of reorientation in the inequant shaped grain aggregates is not as extensive as in the polycrystalline aggregate as pointed out by Wilson (1986).

Fluid production and migration

Evidence for the transformation of the solid phase into a fluid is the presence of birefringence changes either within a grain (see grain d, Fig. 2b) or along grain boundaries (Fig. 2a) and also by the presence of small isotropic regions within a grain. Melting initially began in individual grains (grains a and d, Fig. 2) but progressively spreads into neighbouring grains. The distribution of the melt front in any particular grain is dependent on both the grain shape and in part on its crystallographic orientation with respect to neighbouring grains. The local orientation control on the development of partial melts is clearly seen in the more elongate grains (such as grain a, Fig. 2), where melting spreads from the elongate grain into neighbouring grains that have similar orientations. These melt regions are observed to progressively enlarge as the melting process proceeds (e.g. area d, Figs. 2b & c). This process of melting is essentially one of localized melt thinning of the sample as seen by the birefringe fringe that forms around the melted region (area a, Figs. 3d–f). Where the melt develops, small pockets of fluid are preserved within the polycrystalline framework.

In the sample where there was an anisotropy in the initial grain shape (Fig. 2), distinct mechanical contrasts between the solid portion and the melt became obvious. An early left-lateral displacement of the layering and grain boundaries develops (arrows at e in Fig. 2b) which progressively becomes a discontinuity that separates a melted region (f in Fig. 2f) from the solid grain framework. The shear is approximately parallel to one of the planes of maximum shear stress (cf. slip-lines in Fig. 4a), and produces a small amount of extrusion of the unconfined lateral boundary of the sample. To accommodate this displacement, there is a complementary right-lateral rotation of the layering along the other zone of maximum shear stress. This produces a kinking of the ice lattice, similar to that described by Wilson *et al.* (1986). The melt, and hence fluid distribution, in these experiments is characterized by the occurrence along zones inclined parallel to the zone of high resolved shear stress and in pools adjacent to the fixed platen. Figure 3(g) illustrates the obvious melt distribution prior to crystallization.

In the polycrystalline aggregate, the first melt was observed adjacent to the fixed platen (a in Fig. 3d). The melt penetrates and spreads along grain boundaries with the consumption of the adjacent solid phase to form a melt pool. Simultaneously, further melt pockets were initiated (e.g. b, c and d in Fig. 3e) that again expanded by a process of melt thinning along grain boundaries and eventually formed interconnected pools of melt (Fig. 3f). The distribution of melts in the polycrystalline ice appears to be closely related to the slip-line field for a typical plane strain deformation (Fig. 4b) and lie close to planes of maximum resolved shear stress. Melt is never observed in the triangular area (ACB) between the set of conjugate slip-lines (Fig. 4b).

Crystal growth

The location of the fluid-filled regions can be seen quite clearly in Figs. 2(g) and 3(g) as discrete areas bounded by the interlocking framework of deformed grains. It can be observed that during the nucleation phase (Figs. 2h and 3h) numerous microscopic crystals grew perpendicular or at a high angle to grain boundaries that abut the fluid. The ice first appears as elongate skeletal crystals forming a fretwork which locally encloses the fluid. There is fast lateral growth of these crystals with an orientation comparable to that of the host grain. The phase transformation from fluid to crystal takes place heterogeneously on the face of the adjoining crystal mass or on the wall of silicon oil that contains the fluid. Therefore, within the fluid regions, there are regions of microscopic crystals that have a variety of different orientations. As the crystals continue to grow from the fluid (Figs. 2j & k) in different directions, they encroach on one another to form a touching framework (Fig. 2l). The effect of encroachment of adjacent grains or multiples of growing grains is to form a larger grain (Fig. 2m).

Immediately after the inhibition of lateral growth, there is further coalescence of adjacent grains and the thickening of the elongate crystals. The thickening of the grain is seen in a progressive increase (Figs. 2j–m) in the birefringence colours and produces an interlocking grain aggregate (Fig. 2m) generally composed of irregular shaped crystals. Because of the anisotropic growth kinetics and competitive growth between neighbouring grains, there is a tendency for the grains to grow more rapidly along their length than width, as described by Ketcham & Hobbs (1967).

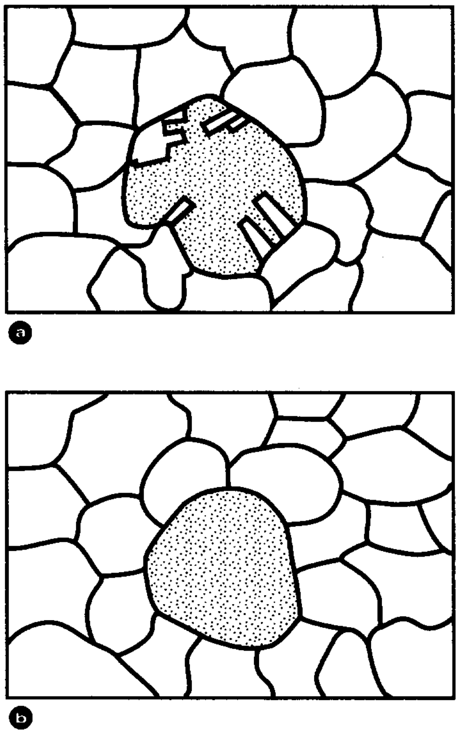

Fig. 5. Microstructures that relate to fluid inclusions (a) during the crystal growth process euhedral crystals grow into the fluid inclusion. (b) Modification of this texture occurs as the crystal aggregate accommodates the imposed stress field. The interface between the fluid and crystal matrix adjusts with the removal of all evidence of pre-existing euhedral crystals.

Crystallization under static conditions

Crystallization under static conditions was achieved by restricting motion of the moving platen, by turning off the motor prior to the onset of crystallization (Fig. 2h). This meant that there was no macroscopic deviatoric stress acting on the fluid or growing crystals up to the stage where the crystals formed the touching framework. The resulting crystal growth (Fig. 2h) produced many near equant to tabular ice crystals (Fig. 2i); skeletal ice crystals are rare at the termination of the crystal growth process. The size of the crystals in the fretwork also varied and appeared to be sensitive to the number of nuclei. As the number of nuclei increases, the size decreases. During the crystal growth process, coalescence of similarly oriented neighbouring nuclei occurred (e.g. Figs. 2j–m) and this also contributed to the final size, shape and number of tabular grains distributed in the final solid phase.

Crystallization under dynamic conditions

At first, the skeletal crystals showed a range of orientation with respect to the shortening axis (Figs. 3g & h) but in general they tended to be more or less aligned parallel to the slip-lines. As the experiments progressed, there was a very fast elimination of skeletal crystals immediately upon the formation of the touching framework (Fig. 3i). The skeletal and tabular crystals that had grown from the fluid became deformed and immediately produced irregular and equiaxed grains that rapidly evolved into a serrated interlocking grain structure. This grain structure also progressively changed orientation, seen from birefringence changes (Figs. 3h & i) and was incorporated into the adjacent polycrystalline aggregate. At the same time, there was a complete elimination of any microstructure which would have suggested the existence of large areas of fluid in this polycrystalline aggregate (Fig. 3j).

The only evidence for the existence of the fluid phase in the final polycrystalline grain aggregates was the development of small droplets of immiscible silicon oil (arrows in Fig. 3j), used as a lubricant between the sample and coverglass. At the time of initial crystallization, a small pool of silicon oil, or residual fluid, formed between the growing crystals due to compositional variaton. In some droplets, the tips of the growing crystals extended beyond the droplet boundary into the pool. Initially, these elongate crystal tips were the only evidence for crystal nucleation. As the sample underwent further deformation, even these crystals were eliminated by grain boundary adjustments in the adjacent polycrystalline aggregate and a change of geometry occurred at the interface between the fluid inclusion and its host grains (Fig. 5). The initial surface energies that controlled the euhedral crystal shapes were obviously overcome by the attempt of the grain aggregate to reduce the surface boundary energy of the fluid inclusion to a minimum. In the process, there was elimination of all textural evidence for crystal growth from a fluid phase.

THE EFFECT OF STRAIN ON THE INITIATION OF MELTING

In these experiments, it is obvious that the non-homogeneous plane strain deformation observed in this perfectly-plastic solid approximates that specified by the slip-line field theory (Johnson & Mellor 1973). Similarly, the spatial relationship between the initial distribution of melt sites and slip-line vectors (Fig. 4b) suggests that the melt formation is related and is discussed in greater detail by Wilson *et al.* (in press). These slip-lines would pass through the coarse-grained aggregate and the plastic work done in the shearing process would be almost entirely dissipated in individual grains as heat.

The localized increase in the free-energy would be due to: (1) the intragranular lattice defect energy; (2) the localized elastic energy that would correspond to the yield stress associated with the slip-lines (Johnson & Mellor 1973); and (3) a minor contribution of the surface free energy (Jurewicz & Watson 1984) that relates to processes occurring on the grain boundaries. Because ice is a very poor heat conductor, and the experiment was maintained at a constant temperature, then loss of this heat to adjacent areas through conduction is probably minimal and explains the localization of the melt. These high strain zones with increased strain energy levels are the sites where the activation energy for the ice to water phase transition is overstepped and the first melt production occurs.

New nucleation sites continued to be located along the sites of the slip-lines. Once the melting started in these zones, it continued to be the preferred site as this is presumably the area where strain was concentrated, hence, a zone of increased strain energy. As the plastic deformation continues, the melt had a strain weakening effect, and therefore enhanced strain localization.

The solid or liquid suspension will only have a macroscopic yield stress for plastic deformation if the volume fraction of solids is sufficient to form a touching framework. For a suspension of fluid and crystals to have a yield stress, it must be capable of supporting a small, non-zero stress without deforming continuously. The macroscopic stress can be supported if there is the crystal framework that is unable to move relative to another due to its orientation rigidity or small volume of melt. Conversely, if the growing crystals are not in contact and have the geometric freedom to move relative to each other, then there is no kinematic reason why they should not be subjected to an applied macroscopic stress. Such a suspension may have a large apparent viscosity but will not have a yield strength.

MODEL FOR CRYSTALLIZATION IN A STRESS FIELD

There is an obvious need for a simple model which can describe the texture in a single-stage opening vein system. These experiments are examples of a situation where there is an absence of episodic fracturing events that are synchronous or post-date crystal growth. In these experiments, the deformed aggregate was melted for short enough times so that the unmelted remnants or substrate remained as nucleation surfaces for subsequent crystal growth. No further plastic deformation features developed in the solid phase while any appreciable quantity of fluid existed. Instead displacements occurred between the solid phases through the movement of the intervening fluids. The crystallization of the initially homogeneous fluid in the dilational openings created by the melting produced two fundamentally different textures or grain microstructures that are a function of the nature of the imposed macroscopic deviatoric stress.

It is clear that nucleation events that closely follow melting are heterogeneous. In all cases the sites for nucleation within the fluid region were provided by the pre-existing marginal solid phase (Fig. 6a). The growth of a crystal from the fluid is dependent on the crystal lattice orientation. As ice has a markedly lower surface energy parallel to (0001) (Ketcham & Hobbs 1967) this is the face that is dominantly developed during the initial stages of crystallization. The growth of these crystals is anisotropic (Fig. 6b) and under static loading conditions the *face-free growth* of these crystals and the consumption of the fluid produces an aggregate of elongate crystals that have well-defined dihedral angles at the termination of each crystal (Fig. 6c). Therefore, in the statically crystallized grains, the solid aggregate and the few fluid-filled pores develop a morphology that is governed by the local surface energy equilibrium and is quite independent of the macroscopic stress conditions.

In the dynamically crystallized aggregate the initial crystal growth develops a framework between which there is a network of isolated and interconnected areas that contain fluid (Fig. 6d). In this situation, the local macroscopic stresses related to crystal growth are exceeded by the macroscopic stress as the solid crystals begin to support the load across grain contacts. At the same time, the interstitial fluid is hydrostatically stressed (Fig. 6d) so that local deviatoric stress differences will arise between the crystal grain contact and the fluid. Crystal–crystal interfaces will support much higher normal stresses, and possible shear stress as well. The overall effect is a highly anisotropic and inhomogeneous stress at the sites of *contact growth* with the initiation of solid state recrystallization (Fig. 6e).

The solid-state recrystallization in the contact growth model involves fast migration of boundaries that presumably initiates with the lowering of the free energy produced by elastic distortion as deformation is transmitted across the impinging framework. Crystallographic fabrics recorded during ice experiments (Wilson 1986) suggest that the growing grains are typically characterized by having the major slip systems parallel to an orientation of maximum resolved shear stress. This is probably the reason why the ice produces identical patterns of crystallographic orientation in the wallrock and in the recrystallized cavity. This suggests that the grain boundary migration is initially driven by variations in strain energy that reflect the plastic anisotropy of the ice. Once an orientation favourable for single slip is created the grain will continue to deform, but it will tend to deform relatively homogeneously. Because there is no tendency to undergo multislip, it is conceivable that the deformed grain will have a low internal elastic distortional energy and grain boundary migration driven by the generation of dislocations will begin to slow. At this stage grain boundary energies provided by a grain's radius of curvature, will become the main driving force. The motion of the boundary will be restricted by the

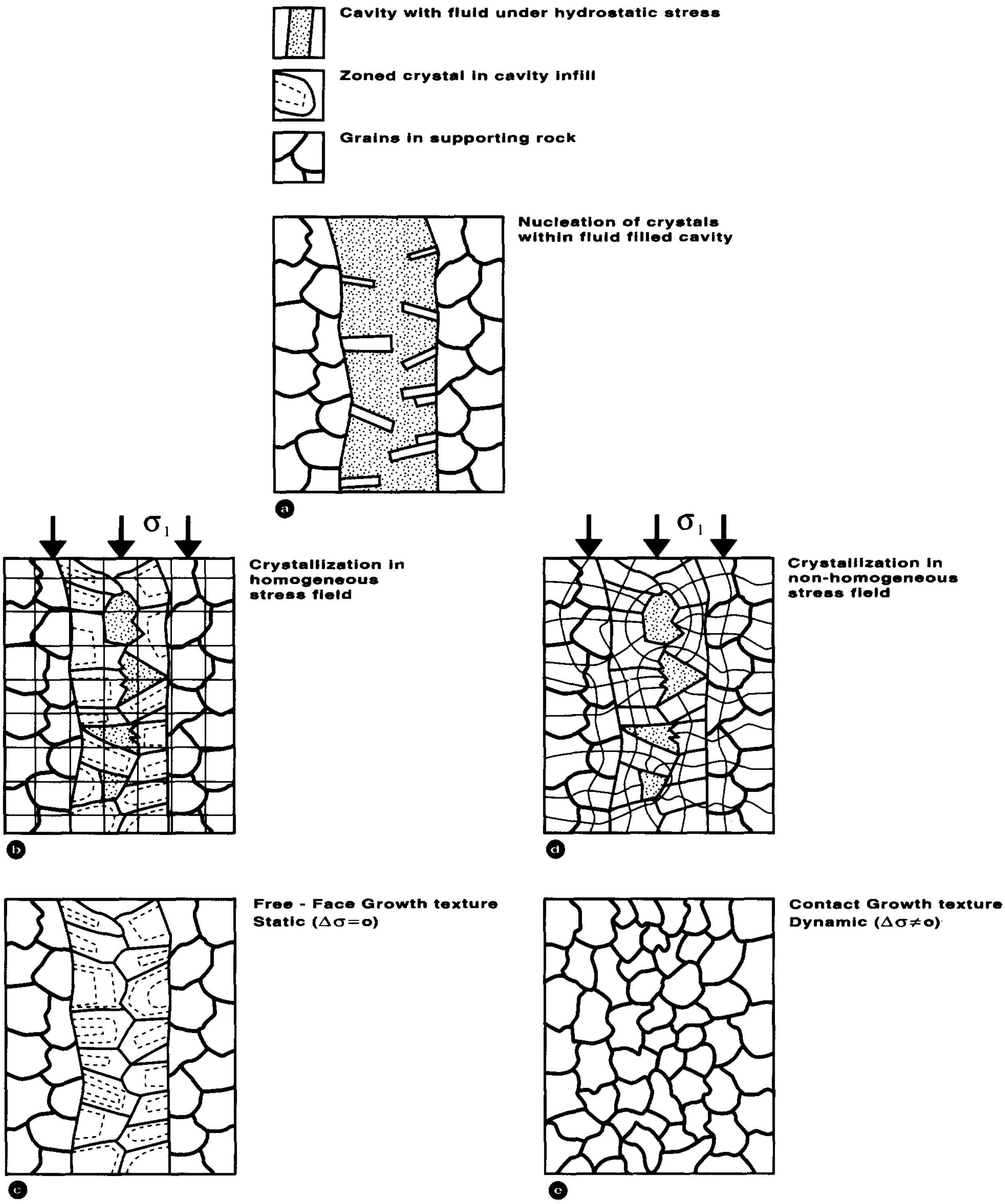

Fig. 6. Progressive stages in the sealing of a vein under static (b&c) and dynamic conditions (d&e). (a) Crystal–fluid existing in a cavity within a deformed aggregate of grains where the initial crystal orientation is determined in part by the shape of the boundary walls of the cavity. (b) Crystal–crystal–fluid where the shape and rate of growth of the crystal from the wall is determined by the magnitude of surface energies on faces of different orientations. This rock can support a macroscopic stress that is nearly equal to the fluid pressure. (c) Termination of growth in a homogeneous stress field or under static conditions. (d) Crystal–crystal–fluid mixture that is supporting a greater load than the fluid in its pores where grain boundaries cannot sustain a shear stress. (e) Termination of growth in a non-homogeneous stress field.

misorientation of the grains relative to each other and by the available elastic strain energy and temperature.

Hence, the primary factor that governs the microstructure appears to be transmission of a macroscopic stress. With no deviatoric stress (free-face growth model; Fig. 6c), the microstructures are a complex intergrowth of melt-grown crystals within a recrystallized grain aggregate that has had a prior history of plastic deformation. Textures such as these are commonly reported in hydrothermal quartz veins (Stel 1981). However, there is also the interplay of density of nuclei, shape of the cavity, crystallization rate and, to some degree, the growth rate and this is particularly important in the formation of crack–seal veins and has been described by Urai *et al.* (1991). In the contact growth model (Fig. 6e) there was no transmission of a macroscopic stress where any applicable quantities of fluid existed. It was only after there was both terminal and lateral impingement of the crystals that there was full restoration of a uniformly distributed stress field across the grain aggregate. In the intervening stage (Fig. 6d) impinging crystals could interact and plastic deformation was accommodated mainly through grain boundary migration. This is a solid-state process driven by a reduction of internal strain energy developed in the impinging grains. Hence, it is the kinematic environment that probably controls the recrystallization phenomenon. The resulting metamorphic texture produced by the contact growth model becomes indistinguishable from the host in both grain shape and lattice preferred orientation.

COMPARISON TO NATURAL VEIN TEXTURES

The findings of these experiments and the proposed models have applications to natural vein systems in metamorphic rocks that have not undergone subsequent intragranular deformation. The morphology of many vein systems developed in compressional environments include large, clear interlocking crystals that appear to grow in open fractures (Fig. 1). The strain free crystals in these veins, that grow directly from the fluid, can be identified by the contrast in their grain size and composition from the wallrocks and by the presence of an internal concentric zoning (Fig. 1a). The zoning, defined by arrays of fluid or mineral inclusions, often parallel to euhedral terminations, or crystallographic planes can be observed optically or highlighted using cathode luminescence techniques (Stel 1981, Urai *et al.* 1991). Veins composed of and dominated by such crystals have anhedral crystal shapes with clear crystal terminations (Fig. 1b), show considerable variation in orientation and grain size (Fig. 1c), and would therefore evolve through processes similar to those described in the free-face growth model (Fig. 6c). They would grow in a static environment to produce anhedral and prismatic crystals (Table 1) that abut distinct discontinuities or demarcations in textures from the adjacent wallrock. Such vein infills lack intracrystalline deformation effects that can be attributed to plastic deformation and as such can only develop from crystal growth from a fluid in a free space. These veins contrast markedly to the recrystallized textures that originate from later imposition of overprinting deformations. The latter are distinguished by varying microstructures that include deformation lamellae associated with a mixture of recovery and dynamic recrystallization features such as deformation bands, subgrains and recrystallized grains.

Other natural vein infills can be composed almost entirely of coarse recrystallized polygonal grain aggregates that are not associated with intracrystalline deformation features (Fig. 1d). The dihedral angles between grain boundaries observed in such strain-free aggregates suggests that the grains are in textural equilibrium. Grain size variations may be observed across a vein, while still maintaining equilibrium dihedral angles, and such grains may exist next to zoned anhedral crystals or co-exist within other grain morphologies, such as the antitaxial crack–seal vein microstructures as illustrated by Cox (1987, fig. 1). These polygonal grains seem to be best explained with the dynamically recrystallized contact growth model where the pre-existing growth texture is destroyed by grain boundary migration. The grain size variation across the polygonal grain aggregate may, in fact, reflect the rate of grain boundary migration in

Table 1. Schematic relationship between regime of vein formation, textures and processes that contribute to a particular vein type. Such vein types can be recognized in deformed rocks that are uncomplicated by superimposed deformation events

Regime of vein formation	Kinematic environment	Typical textures	Mechanism	Type of vein infill
1. Growth from fluid filled cavity in equilibrium with the local stress	Static	Euhedral, prismatic	Free-face growth displaces fluid	Cavity infill (buck or comb)
2. Growth from fluid filled cavity in presence of deviatoric stress	Syntectonic	Irregular and metamorphic	Contact growth and solid-state recrystallization	Anhedral and recrystallized
3. Growth in solid grain aggregate in presence of deviatoric stress	Syntectonic	Fibrous	Incremental microcracking followed by sealing due to precipitation from fluid	Crack–seal
4. Growth in solid grain aggregate in absence of deviatoric stress	Static	Anhedral or prismatic	Chemical or polymorphic replacement of existing grain structure	Replacement

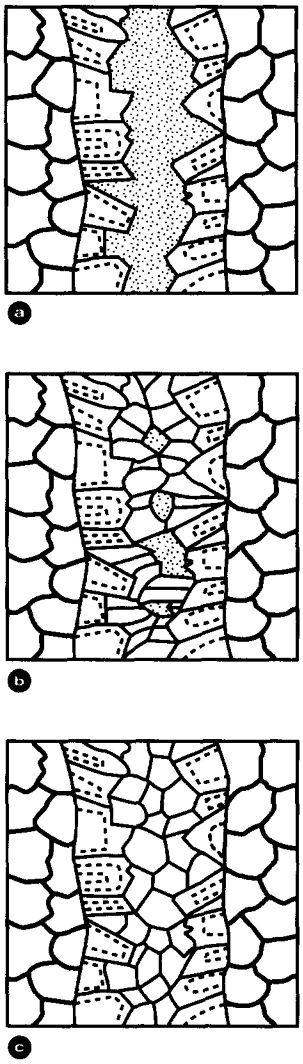

Fig. 7. Schematic sketch illustrating the evolution of a composite vein composed of free-face growth and contact growth textures. (a) Free-face growth; (b) impinging system of crystals–fluid; and (c) free-face and contact growth texture.

response to internal strain energy distribution or the role of impurities in pinning and restricting the migration of grain boundaries.

The composite veins that are composed of both anhedral and irregular metamorphic textures (Table 1) may involve two or more stages of crystal growth that reflect changes in the physical environments. The development of anhedral grains adjacent to the vein walls would probably proceed by processes of free-face growth into a static fluid (Fig. 7a). This would be followed by a cessation in crystal growth or change in the nature or physical condition of the fluid flux. For example, there may be a switch to turbulent flow with the further propagation of the vein. Either way a secondary nucleation stage would occur and embryonic crystals would begin to nucleate and may soon form a touching framework that would allow contact growth and syntectonic recrystallization to develop. At this stage elastic stresses will build up and be distributed so that the normal stress varies along each touching grain boundary whilst still maintaining a hydrostatic state of (macroscopic) stress on the scale of many grains (Fig. 7b). The resulting microstructure would be a mixture of irregular and metamorphic textures (Fig. 7c). In the experiments described in this paper, such a two-stage process was not observed as no fluid flow existed in the samples. However, in other experiments (Sunagawa 1990) and situations where there is fluid movement, the two-stage process of free-face and contact growth (Fig. 7) does involve a secondary nucleation stage that produces the contrasting crystal types.

The possible variations in vein microstructures are many, but for a single phase crystallization there are restrictive patterns that can develop depending on the nature of the opening and macroscopic stress regime. The absence of inclusion trails and laminations in a vein tends to suggest an absence of incremental opening, as in the crack–seal model (Ramsay 1980). If a fracture evolves as a single-stage opening in a compressional environment, such as in a *shear vein* array, then there is an excellent possibility that the composite vein microstructure will be dominated by free-face and contact growth textures. The dilational opening would first originate through rapid decompression and the vein would be held open by high fluid pressures, this may involve turbulent fluid flow but, once infilling commences, the crystal framework would not be capable of supporting the macroscopic stresses without deforming the infill. The ensuing syntectonic deformation will produce a microstructure that involves both anhedral and metamorphic textures (Table 1).

Crack–seal veins characterized by fibrous infills are always syntectonic (Table 1), for instance, the formation of syntaxial or antitaxial veins (Durney & Ramsay 1973) where the crystal infill is initially accreted either on the wall or in the centre of the vein. This process may be repeated a number of times as individual extensional events occur. Such a crystal framework would be dominated by the macroscopic stress at the boundary between the solid grain aggregate and the crystallized phase. Unlike the syntectonic growth from a fluid-filled cavity, significant volumes of fluid may not exist at this interface as diffusive accretionary processes will contribute to the addition of material (Durney & Ramsay 1973, Ramsay 1980). Replacement veins (Table 1), on the other hand, can be distinguished from the two principal vein types described in this paper on the basis that the texture preserves evidence of the pre-existing rock structure that the infilling material overgrows.

COMPARISON WITH TEXTURES IN ANATECTIC MELT SEGREGATIONS

Direct comparison with leucosome generation is difficult because many natural leucosomes, produced by metamorphic melt reactions, involve multicomponent mineral systems in comparison to the single phase used in these experiments. The melt may also preserve reactions such as corroded grains, precipitation of interstitial melt phases and the presence of metamorphic sympletic intergrowths (e.g. Hand & Dirks 1992). Similarly, many leucosomes may involve subsolidus reactions (Sawyer 1987) and are extensively modified by the later deformation or involve melt remobilization. The presence of submicroscopic heterogeneous nucleation sites within an anatectic melt means that many mineral phases can be isolated within the melt. These grains which may be minor phases would never form a touching framework and may not exhibit syntectonic deformation features. Hence, they would preserve growth textures and exhibit different mechanical properties from the rest of the crystallizing melt phase. However, there are direct geometrical and microstructural comparisons that can be made between a typical anatectic vein system in a natural rock and model system described here.

The results of these experiments demonstrate that the shape and the distribution of a melt region is closely aligned to strain localization. This localization can be related to slip-lines where plastic strain creates a two-dimensional network of melt. This corresponds to the observation that in natural rocks many leucosomes are generated under a distinct compressional regime and can be correlated with zones of high plastic strain (e.g. Hand & Dirks 1992). However, these experiments were not able to demonstrate how a partial melt may separate itself from the supporting matrix grains.

Microstructural observations of many natural anatectic vein systems suggest that there may be little difference in grain shape and grain size from the vein interior to the mineral framework in the wallrocks. The main minerals infilling these veins generally include syntectonic deformational features, grain shapes reflecting grain boundary adjustments between neighbouring mineral phases (e.g. McLellan 1988) and strain-free grains with polygonal shapes and equilibrium grain boundaries (e.g. Hand & Dirks 1992). Deformation induced recrystallization can produce these optically strain-free grains shortly after the time of vein emplacement through processes similar to the contact growth model described in this paper. This is quite different from what is expected for free-face growth of these minerals in a fluid filled cavity as in the model of Sawyer (1987). It is suggested therefore that the apparent absence of pre-existing crystal growth morphologies found in the majority of metamorphic terrains is probably a direct consequence of a deviatoric stress being transmitted by the impinging crystal framework. The effect of the stress on the crystal nuclei within the vein would be to immediately deform the crystals to produce metamorphic textures.

CONCLUSIONS

By observing the microstructure of crystal aggregates, crystal habit and the internal heterogeneity, it is possible to analyse the growth or post-growth histories of single and multiple stages in a vein infilling. Based on evidence from these ice analogue experiments it is possible to suggest that intragranular nucleation and subsequent growth of a crystalline phase as a cavity infill microstructure is only preserved where the macroscopic deviatoric stress is insufficient to cause further deformation. Where a cavity infill contains a crystal framework that is capable of transmitting a deviatoric stress then the resulting ductile deformation will produce recrystallization features in the crystallizing phase. Hence, if such microstructures are recognized in a vein structure, they may imply the nature of the stress field after the propagation of the fracture that produces the cavity.

Hence, the presence of a deviatoric stress is extremely important in the crystallization of a crystal from a fluid-filled vein and plays a significant role in the development of the texture that may influence further fluid flow and the mechanical behaviour of a vein. In a static regime, small amounts of the fluid will be trapped and preserved as fluid inclusions within the growing crystal and their distribution within a grain can allow one to distinguish free-face growth from crack–seal veins. The crystal texture in the free-face growth environment will be more open with large variations in dihedral angles that would allow the passage of further metamorphic fluids. However, in the dynamic regime, the fluid will not be trapped in the grains, instead it will be swept into the boundaries of coarse grains that have an equilibrium microstructure and lacks intracrystalline deformation. This texture may seal the vein and impede further fluid flow within the grain aggregate. Such a metamorphic vein, for example, an anatectic melt segregation becomes indistinguishable in texture and mechanical properties from the enclosing wallrocks and responds to the stress field, not as a discontinuity, but as a passive marker within the bulk rock.

Acknowledgements—This work was supported financially by the Australian Research Council. The Glaciology Section of the Australian Antarctic Division is thanked for the maintenance of the coldroom facilities where experiments and specimen preparation were undertaken. Thomas Will is thanked for his comments on the initial draft of this manuscript.

REFERENCES

Beach, A. 1977. Vein arrays, hydraulic fractures and pressure solution structures in a deformed flysch sequence. S.W. England. *Tectonophysics* **40**, 201–225.

Cox, S. F. 1987. Antitaxial crack–seal vein microstructures and their relationship to displacement paths. *J. Struct. Geol.* **9**, 779–787.

Downing, K. & Morrison, G. 1989. Application of quartz-textures to the classification of gold deposits using North Queensland examples. *Econ. Geol. Monogr.* **6**, 342–355.

Durney, D. W. & Ramsay, J. G. 1973. Incremental strains measured by syntectonic crystal growths. In: *Gravity and Tectonics* (edited by De Jong, K. A. & Scholten, R.). John Wiley, New York, 67–96.

Etheridge, M. A. 1983. Differential stress magnitudes during regional deformation and metamorphism—upper bound imposed by tensile fracturing. *Geology* **11**, 231–234.

Johnson, W. & Mellor, P. B. 1973. *Engineering Plasticity*. Van Nostrand Reinhold, New York.

Jurewicz, S. R. & Watson, E. B. 1984. Distribution of partial melt in a felsic system: The importance of surface energy. *Contr. Miner. Petrol.* **85**, 25–29.

Ketcham, W. M. & Hobbs, P. B. 1967. The preferred orientation in the growth of ice from the melt. *J. Crystal Growth* **1**, 263–270.

Hand, M. & Dirks, P. H. G. M. 1992. The influence of deformation on the formation of axial-planar leucosomes and the segregation of small melt bodies within the migmatitic Napperby Gneiss, Central Australia. *J. Struct. Geol.* **14**, 591–604.

Holness, M. B. & Graham, C. M. 1991. Equilibrium dihedral angles in the system H_2O–CO_2–NaCl; calcite, and implications for fluid flow during metamorphism. *Contr. Miner. Petrol.* **108**, 368–383.

McLellan, E. L. 1988. Migmatite structures in the central gneiss complex, Boca de Quadra, Alaska. *J. metamorph. Geol.* **6**, 517–542.

Ramsay, J. G. 1980. The crack–seal mechanism of rock deformation. *Nature* **284**, 135–139.

Sawyer, E. W. 1987. The role of partial melting and fractional crystallization in determining discordant migmatite leucosome compositions. *J. Petrol.* **28**, 445–473.

Stel, H. 1981. Crystal growth in cataclasites: Diagnostic microstructures and implications. *Tectonophysics* **78**, 585–600.

Sunagawa, I. 1990. *In situ* observation of nucleation, growth and dissolution of crystals in ordinary temperature aqueous solutions and high temperature silicate solutions. In: *Dynamic Processes of Material Transport and Transformation in the Earth's Interior* (edited by Marumo, F.). Terra Scientific, Tokyo, 139–168.

Tapponnier, P. & Molnar, P. 1976. Slip line field theory and large scale continental tectonics. *Nature* **264**, 319–324.

Urai, J. L., Williams, P. F. & van Roermund, H. L. M. 1991. Kinematics of crystal growth in syntectonic fibrous veins. *J. Struct. Geol.* **13**, 823–836.

Wheeler, J. 1991. A view of texture dynamics. *Terra Nova* **3**, 123–136.

Wilson, C. J. L. 1981. Experimental folding and fabric development in multilayered ice. *Tectonophysics* **78**, 139–159.

Wilson, C. J. L. 1984. Shear bands, crenulations and differentiated layering in ice–mica models. *J. Struct. Geol.* **6**, 303–319.

Wilson, C. J. L. 1986. Deformation induced recrystallization of ice: The application of in situ experiments. In: *Mineral and Rock Deformation—Laboratory Studies* (edited by Hobbs, B. E. & Heard, H. C.). *Am. Geophys. Un. Geophys. Monogr.* **36**, 213–232.

Wilson, C. J. L., Burg, J.-P. & Mitchell, J. C. 1986. The origin of kinks in polycrystalline ice. *Tectonophysics* **127**, 27–48.

Wilson, C. J. L., Zhang, Y. & Stüwe, K. In press. Deformation enhanced melting in ice. *Cold Regions Sci. & Technol.*